

Can We Solve 3D Vision Tasks Starting from A 2D Vision Transformer?

Anonymous authors
Paper under double-blind review

Abstract

Vision Transformers (ViTs) have proven to be effective, in solving 2D image understanding tasks by training over large-scale image datasets; and meanwhile as a somehow separate track, in modeling the 3D visual world too such as voxels or point clouds. However, with the growing hope that transformers can become the “universal” modeling tool for heterogeneous data, ViTs for 2D and 3D tasks have so far adopted vastly different architecture designs that are hardly transferable. That invites an (over-)ambitious question: *can we close the gap between the 2D and 3D ViT architectures?* As a piloting study, this paper demonstrates the appealing promise to understand the 3D visual world, using a standard 2D ViT architecture, with only minimal customization at the input and output levels without redesigning the pipeline. To build a 3D ViT from its 2D sibling, we “inflate” the patch embedding and token sequence, accompanied with new positional encoding mechanisms designed to match the 3D data geometry. The resultant “minimalist” 3D ViT, named **Simple3D-Former**, performs surprisingly robustly on popular 3D tasks such as object classification, point cloud segmentation and indoor scene detection, compared to highly customized 3D-specific designs. It can hence act as a strong baseline for new 3D ViTs. Moreover, we note that pursuing a unified 2D-3D ViT design has practical relevance besides just scientific curiosity. Specifically, we demonstrate that Simple3D-Former naturally is able to exploit the wealth of pre-trained weights from large-scale realistic 2D images (e.g., ImageNet), which can be plugged into enhancing the 3D task performance “for free”.

1 Introduction

In the past year, we have witnessed how transformers extend their reasoning ability from Natural Language Processing(NLP) tasks to computer vision (CV) tasks. Various vision transformers (ViTs) (Carion et al., 2020; Dosovitskiy et al., 2020; Liu et al., 2021b; Wang et al., 2022) have prevailed in different image/video processing pipelines and outperform conventional Convolutional Neural Networks (CNNs). One major reason that accounts for the success of ViTs is the self-attention mechanism that allows for global token reasoning (Vaswani et al., 2017b). It receives tokenized, sequential data and learns to attend between every token pair. These pseudo-linear blocks offer flexibility and global feature aggregation at every element, whereas the receptive field of CNNs at a single location is confined by small size convolution kernels. This is one of the appealing reasons that encourages researchers to develop more versatile ViTs, while keeping its core of self-attention module simple yet efficient, e.g., Zhou et al. (2021); He et al. (2021).

Motivated by ViT success in the 2D image/video space, researchers are expecting the same effectiveness of transformers applied into the 3D world, and many innovated architectures have been proposed, e.g., Point Transformer (PT, Zhao et al. (2021)), Point-Voxel Transformer (PVT, Zhang et al. (2021)), Voxel Transformer (VoTr, Mao et al. (2021)), M3DETR(Guan et al., 2021). Although most of the newly proposed 3D Transformers have promising results in 3D classification, segmentation and detection, they hinge on heavy customization beyond a standard transformer architecture, by either introducing pyramid style design in transformer blocks, or making heavy manipulation of [self-attention](#) modules to compensate for sparsely-scattered data. [Consequently, ViTs for same type of vision tasks under 2D and 3D data is difficult to share similar architecture designs.](#) [On the other hand, there are recently emerged works, including Perceiver](#)

IO(Jaegle et al., 2021a), and SRT(Sajjadi et al., 2022), that make fairly direct use of ViTs architecture, with only the input and output modalities requiring different pre-encoders.

That invites the question: *are those task-specific, complicated designs necessary for ViTs to succeed in 3D vision tasks? Or can we stick an authentic transformer architecture with minimum modifications, as is the case in 2D ViTs?* Note that the questions are of both scientific interest, and practical relevance. On one hand, accomplishing 3D vision tasks with standard transformers would set another important milestone for a transformer to become the universal model, whose success could save tedious task-specific model design. On the other hand, bridging 2D and 3D vision tasks with a unified model implies convenient means to borrow each other’s strength. For example, 2D domain has a much larger scale of real-world images with annotations, while acquiring the same in the 3D domain is much harder or more expensive. Hence, a unified transformer could help leverage the wealth of 2D pre-trained models, which are supposed to learn more discriminative ability over real-world data, to enhance the 3D learning which often suffers from either limited data or synthetic-real domain gap. Other potential appeals include integrating 2D and 3D data into unified multi-modal/multi-task learning using one transformer (Akbari et al., 2021).

As an inspiring initial attempt, 3DETR (Misra et al., 2021) has been proposed. Despite its simplicity, it is surprisingly powerful to yield good end-to-end detection performance over 3D dense point clouds. The success of 3DETR implies that the reasoning ability of a basic transformer, fed with scattered point cloud data in 3D space, is still valid even without additional structural design. However, its 2D siblings, DETR(Devlin et al., 2019), cannot be naively generalized to fit in 3D data scenario. Hence, 3DETR is close to a universal design of but without testing itself over other 3D tasks, and embrace 2D domain. Moreover, concurrent works justify ViT can be extended onto 2D detection tasks without Feature Pyramid Network design as its 2D CNN siblings (Chen et al., 2021; Fang et al., 2022; Li et al., 2022), **leading** a positive sign of transferring ViT into different tasks. Uniform transformer model has been tested over multimodal data, especially in combination with 1D and 2D data, and some 3D image data as well (Jaegle et al., 2021b; Girdhar et al., 2022).

Therefore, we are motivated to design an easily customized transformer by taking a **minimalist** step from what we have in 2D, i.e., the standard 2D ViT (Dosovitskiy et al., 2020). The 2D ViT learns patch semantic correlation mostly under pure stacking of transformer blocks, and is well-trained over large scale of real-world images with annotations. However, there are two practical gaps when **bringing** 2D ViT to 3D space. i) **Data Modality Gaps**. Compared with 2D grid data, the data generated in 3D space contains richer semantic and geometric meanings, and the abundant information is recorded mostly in a spatially-scattered point cloud data format. Even for voxel data, the additional dimension brings the extra semantic information known as “depth”. ii) **Task Knowledge Gaps**. It is unclear whether or not a 3D visual understanding task can gain from 2D semantic information, especially considering many 3D tasks are to infer the stereo structures(Yao et al., 2020) which 2D images do not seem to directly offer.

To minimize the aforementioned gaps, we provide a candidate solution, named as *Simple3D-Former*, to generate 3D understanding starting with a unified framework adapted from 2D ViTs. We propose an easy-to-go model relying on the standard ViT backbone where we made no change to the basic pipeline nor the self-attention module. Rather, we claim that properly modifying (i) positional embeddings; (ii) tokenized scheme; (iii) down-streaming task heads, suffices to settle a high-performance vision transformer for 3D tasks, that can also cross the “wall of dimensionality” to effectively utilize knowledge learned by 2D ViTs, such as in the form of pre-trained weights.

Our Highlighted Contributions

- We propose Simple-3DFormer, which closely follows the standard 2D ViT backbone with only minimal modifications at the input and output levels. Based on the data modality and the end task, we slightly edit only the tokenizer, position embedding and head of Simple3D-Former, making it sufficiently versatile, easy to deploy with maximal reusability.
- We are the first to lend 2D ViT’s knowledge to 3D ViT. We infuse the 2D ViT’s pre-trained weight as a warm initialization, from which Simple-3DFormer can seamlessly adapt and continue training over 3D data. We prove the concept that 2D vision knowledge can help further 3D learning through a unified model.

- Due to a unified 2D-3D ViT design, our Simple3D-Former can naturally extend to some different 3D down-streaming tasks, with hassle-free changes. We empirically show that our model yield competitive results in 3D understanding tasks including 3D object classification, 3D part segmentation, 3D indoor scene segmentation and 3D indoor scene detection, with simpler and more unified designs.

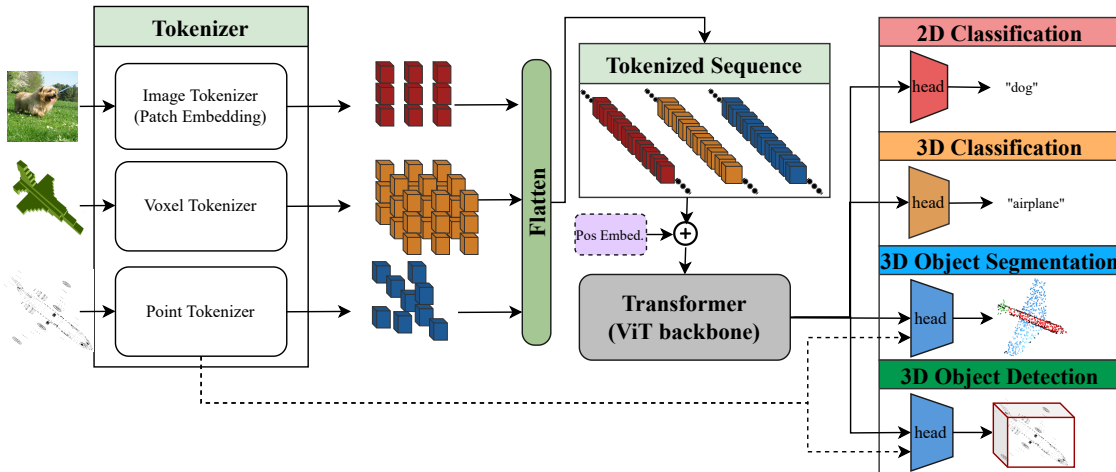


Figure 1: Overview of Simple3D-Former Architecture. As a Simple3D-Former, our network consists of three common components: tokenizer, transformer backbone (in our case we refer to 2D ViT), and a down-streaming task-dependent head layer. All data modalities, including 2D images, can follow the same processing scheme and share a universal transformer backbone. Therefore, we require minimal extension from the backbone and it is simple to replace any part of the network to perform multi-task 3D understanding. Dashed arrow refers a possible push forward features in the tokenizer when performing dense prediction tasks.

2 Related Work

2.1 Existing 2D Vision Transformer Designs

There is recently a growing interest in exploring the use of transformer architecture for vision tasks: works in image generation (Chen et al., 2020a; Parmar et al., 2018) and image classification (Chen et al., 2020a) learn the pixel distribution using transformer models. ViT (Dosovitskiy et al., 2020), DETR (Carion et al., 2020) formulated object detection using transformer as a set of prediction problem. SWIN (Liu et al., 2021b) is a more advanced, versatile transformer that infuses hierarchical, cyclic-shifted windows to assign more focus within local features while maintaining global reasoning benefited from transformer architectures. In parallel, the computation efficiency is discussed, since the pseudo-linear structure in a self-attention module relates sequence globally, leading to a fast increasing time complexity. DeiT (Touvron et al., 2021) focus on data-efficient training while DeepViT (Zhou et al., 2021) propose a deeper ViT model with feasible training. Recently, MSA (He et al., 2021) was introduced to apply a masked autoencoder to lift the scaling of training in 2D space. Recent works start exploring if a pure ViT backbone can be transferred as 2D object detection backbone with minimal modification, and the result indicates it might be sufficient to use single scale feature plus a Vanilla ViT without FPN structure to achieve a good detection performance (Chen et al., 2021; Fang et al., 2022; Li et al., 2022).

2.2 Exploration of 3D Vision Transformers

Transformer is under active development in the 3D Vision world (Fan et al., 2021; 2022). For example, 3D reconstruction for human body and hand is explored by the work (Lin et al., 2021) and 3D point cloud completion has been discussed in (Yu et al., 2021a). Earlier works such as Point Transformer (Engel et al., 2020) and Point Cloud Transformer (Guo et al., 2021) focus on point cloud classification and semantic

segmentation. They closely follow the prior wisdom in PointNet (Qi et al., 2017a) and PointNet++ (Qi et al., 2017b). These networks represent each 3D point as tokens using the Set Abstraction idea in PointNet and design a hierarchical transformer-like architecture for point cloud processing. Nevertheless, the computing power increases quadratically with respect to the number of points, leading to memory scalability bottleneck. Latest works seek an efficient representation of token sequences. For instance, a concurrent work PatchFormer (Cheng et al., 2021) explores the local voxel embedding as the tokens that feed in transformer layers. Inspired by sparse CNN in object detection, VoTR (Mao et al., 2021) modifies the transformer to fit sparse voxel input via heavy hand-crafted changes such as the sparse voxel module and the submanifold voxel module. The advent of 3DETR (Misra et al., 2021) takes an inspiring step towards returning to the standard transformer architecture and avoiding heavy customization. It attains good performance in object detection. Nevertheless, the detection task requires sampling query and bounding box prediction. The semantics contains more information from local queries compared with other general vision tasks in interest, and 3DETR contains transform decoder designs whereas ViT contains transformer encoder only. At current stage, our work focuses more on a simple, universal ViT design, i.e., transformer encoder-based design.

2.3 Transferring Knowledge between 2D and 3D

Transfer learning has always been a hot topic since the advent of deep learning architectures, and hereby we focus our discussion on the transfer of the architecture or weight between 2D and 3D models. 3D Multi View Fusion (Su et al., 2015; Kundu et al., 2020) has been viewed as one connection from Images to 3D Shape domain. A 2D to 3D inflation solution of CNN has been discussed in Image2Point (Xu et al., 2021), where the copy of convolutional kernels in inflated dimension can help 3D voxel/point cloud understanding and requires less labeled training data in target 3D task. On a related note, for video as a 2D+1D data, TimeSFormer (Bertasius et al., 2021) proposes an inflated design from 2D transformers, plus memorizing information across frames using another transformer along the additional time dimension. Liu et al. (2021a) provides a pixel-to-point knowledge distillation by contrastive learning.

It is also possible to apply a uniform transformer backbone in different data modalities, including 2D and 3D images, which is successfully shown by Perceiver (Jaegle et al., 2021b), Perceiver IO (Jaegle et al., 2021a), Omnivore (Girdhar et al., 2022), SVT (Sajjadi et al., 2022), UViM (Kolesnikov et al., 2022) and Transformer-M (Luo et al., 2022). All these works aim at projecting different types of data into latent token embedding but incorporate knowledge from different modalities either with self-attention or with cross-attention modules (with possibly one branch embedding from knowledge-abundant domain). Note that among all these aforementioned work. Only Perceiver discuss the application in point cloud modality with very preliminary result, and Omnivore discuss RGB-D data which is a primary version resembling 3D Voxel data. Contrary to prior works, our Simple3D-Former specifically aims at a model unifying 3D modalities, where point cloud and voxels are two most common data types that has not been extensively discussed in previous universal transformer model design. We discuss in particular how to design 3D data token embeddings as well as how to add 2D prior knowledge. In this paper, we show that with the help of a 2D vanilla transformer, we do not need to specifically design or apply any 2D-3D transfer step - the unified architecture itself acts as the natural bridge.

3 Our Simple3D-Former Design

3.1 Network Architecture

We briefly review the ViT and explain how our network differs from 2D ViTs when dealing with different 3D data modalities. We look for both voxel input and point cloud input. Then we describe how we adapt the 2D reasoning from pretrained weights of 2D ViTs. The overall architecture refers to Figure 1.

3.1.1 Preliminary

For a conventional 2D ViT (Dosovitskiy et al., 2020), the input image $I \in \mathbb{R}^{H \times W \times C}$ is assumed to be divided into patches of size P by P , denoted as $I_{x,y}$ with subscripts x, y . We assume H and W can be divided by P , thus leading to a sequence of length total length $N := \frac{HW}{P^2}$. We apply a *patch embedding* layers

$E: \mathbb{R}^{P \times P} \rightarrow \mathbb{R}^D$ as the tokenizer that maps an image patch into a D -dimensional feature embedding vector. Then, we collect those embeddings and prepend class tokens, denoted as \mathbf{x}_{class} , as the target classification feature vector. To incorporate positional information for each patch when flattened from 2D grid layout to 1D sequential layout, we add a positional embedding matrix $E_{pos} \in \mathbb{R}^{D \times (N+1)}$ as a learn-able parameter with respect to locations of patches. Then we apply L transformer blocks and output the class labeling \mathbf{y} by a head layer. The overall formula of a 2D ViT is:

$$\mathbf{z}_0 = [\mathbf{x}_{class}; E(I_{1,1}); \cdots; E(I_{\frac{H}{P}, \frac{W}{P}})] + E_{pos}; \quad (1)$$

$$\tilde{\mathbf{z}}_l = MSA(LN(\mathbf{z}_{l-1})) + \mathbf{z}_{l-1}; \quad \mathbf{z}_l = MLP(LN(\tilde{\mathbf{z}}_l)) + \tilde{\mathbf{z}}_l; \quad (2)$$

$$\mathbf{y} = h(LN(\mathbf{z}_{L,0})). \quad (3)$$

Here MSA and MLP refer to the multi-head self-attention layer and multi-layer perceptron, respectively. The MSA is a standard qkv dot-product attention scheme with multi-heads settings (Vaswani et al., 2017a). The MLP contains two layers with a GELU non-linearity. Before every block, LayerNorm (LN, Wang et al. (2019a); Baevski & Auli (2019)) is applied. The last layer class token output $\mathbf{z}_{L,0}$ will be fed into head layer h to obtain final class labelings. In 2D ViT setting, h is a single-layer MLP that maps D -dimensional class tokens into class dimensions (1000 for ImageNet).

The primary design principle of our Simple3D-Former is to keep transformer encoder blocks equation 2 same as in 2D ViT, while maintaining the tokenizing pipeline, equation 1 and the task-dependent head, equation 3. We state how to design our Simple3D-Former specifically with minimum extension for different data modalities.

3.1.2 Simple3D-Former of Voxel Input

We first consider the “patchable” data, voxels. We start from the data $V \in \mathbb{R}^{H \times W \times Z \times C}$ as the voxel of height H , width W , depth Z and channel number C . We denote our 3D space tessellation unit as cubes $V_{x,y,z} \in \mathbb{R}^{T \times T \times T \times C}$, where x, y, z are three dimensional indices. We assume the cell is of size T by T by T and H, W, C are divided by T . Let $N = \frac{HWZ}{T^3}$ be the number of total cubes obtained. To reduce the gap from 2D ViT to derived 3D ViT, we provide three different realizations of our Simple3D-Former, only by manipulating tokenization that has been formed in equation 1. We apply a same *voxel embedding* $E_V: \mathbb{R}^{T \times T \times T} \rightarrow \mathbb{R}^D$ for all following schemes. We refer readers to Figure 2 for a visual interpretation of three different schemes.

Naive Inflation One can consider straight-forward inflation by only changing patch embedding to a voxel embedding E_V , and reallocating a new positional encoding matrix $E_{pos,V} \in \mathbb{R}^{(1+N) \cdot D}$ to arrive at a new tokenized sequence:

$$\mathbf{z}_0^V = [\mathbf{x}_{class}; E_V(\mathbf{x}_{1,1,1}); E_V(\mathbf{x}_{1,1,2}); \cdots; E_V(\mathbf{x}_{1,2,1}); \cdots; E_V(\mathbf{x}_{\frac{H}{T}, \frac{W}{T}, \frac{Z}{T}})] + E_{pos,V}. \quad (4)$$

We then feed the voxel tokenized sequence \mathbf{z}_0^V to the transformer block equation 2. The head layer h is replaced by a linear MLP with the output of probability vector in Shape Classification task.

2D Projection (Averaging) It is unclear from equation 4 that feeding 3D tokenized cube features is compatible with 2D ViT setting. A modification is to force our Simple3D-Former to think as if the data were

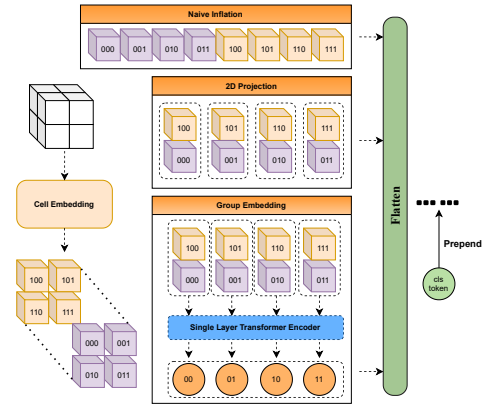


Figure 2: Three different voxel tokenizer designs. The given example is a 2^3 cell division. We number cells for understanding. Top: Naive Inflation; We pass the entire voxel sequence in XYZ coordinate ordering. Middle: 2D Projection; We average along Z -dimension to generate 2D “patch” sequence unified with 2D ViT design. Bottom: Group Embedding; We introduce an additional, single layer transformer encoder to encode along Z -dimension, to generate 2D “group” tokens. Then the flattened tokenized sequence can thereby pass to a universal backbone.

in 2D case, with its 3rd dimensional data being compressed into one token, not consecutive tokens. This resembles the occupancy of data at a certain viewpoint if compressed in 2D, and naturally a 2D ViT would fit the 3D voxel modality. We average all tokenized cubes if they come from the same XY coordinates (i.e. view directions). Therefore, we modify the input tokenized sequence as follows:

$$z_0^V = [\mathbf{x}_{class}; \frac{T}{Z} \sum_{z=1}^{\frac{Z}{T}} E(\mathbf{x}_{1,1,z}); \frac{T}{Z} \sum_{z=1}^{\frac{Z}{T}} E(\mathbf{x}_{1,2,z}); \cdots; \frac{T}{Z} \sum_{z=1}^{\frac{Z}{T}} E(\mathbf{x}_{\frac{H}{T}, \frac{W}{T}, z})] + E_{pos,V}. \quad (5)$$

The average setting consider class tokens as a projection in 2D space, with $E_{pos,V} \in \mathbb{R}^{(1+\tilde{N}) \cdot D}$, $\tilde{N} = \frac{HW}{T^2}$, and henceforth $E_{pos,V}$ attempts to serve as the 2D projected positional encoding with \tilde{N} “patches” encoded.

Group Embedding A more advanced way of tokenizing the cube data is to consider interpreting the additional dimension as a “word group”. The idea comes from group word embedding in BERT-training (Devlin et al., 2019). A similar idea was explored in TimesFormer (Bertasius et al., 2021) for space-time dataset as well when considering inflation from image to video (with a temporal 2D+1D inflation). To train an additional “word group” embedding, we introduce an additional 1D Transformer Encoder(TE) to translate the inflated Z-dim data into a single, semantic token. Denote $\mathbf{V}_{x,y,-} = [\mathbf{V}_{x,y,1}; \mathbf{V}_{x,y,2}; \cdots; \mathbf{V}_{x,y,\frac{Z}{P}}]$ as the stacking cube sequence along z-dimension, we have:

$$\tilde{E}(\mathbf{V}_{x,y,-}) := TE(E(\mathbf{V}_{x,y,-})), \quad (6)$$

$$z_0^V = [\mathbf{x}_{class}; \tilde{E}(\mathbf{V}_{1,1,-}); \cdots; \tilde{E}(\mathbf{V}_{\frac{H}{P}, \frac{W}{P}, -})] + \mathbf{E}_{pos,V}. \quad (7)$$

Here \tilde{E} as a compositional mapping of patch embedding and the 1D Transformer Encoder Layer (TE). The grouping, as an “projection” from 3D space to 2D space, maintains more semantic meaning compared with 2D Projection.

3.1.3 Simple3D-Former of Point Cloud Data

It is not obvious how one can trust 2D ViT backbone’s reasoning power applied over point clouds, especially when the target task changes from image classification to dense point cloud labeling. We show that, in our Simple3D-Former, a universal framework is a valid option for 3D semantic segmentation, with point cloud tokenization scheme combined with our universal transformer backbone. We modify the embedding layer E , positional encoding E_{pos} and task-specific head h originated from equation 1 and equation 3 jointly. We state each module’s design specifically, but our structure does welcome different combinations.

Point Cloud Embedding We assume the input now has a form of (X, P) , $X \in \mathbb{R}^{N \times 3}$, $P \in \mathbb{R}^{N \times C}$, referred as point coordinate and input point features. For a given point cloud, we first adopt a MLP (two linear layers with one ReLU nonlinearity) to aggregate positional information into point features and use another MLP embedding to lift point cloud feature vectors. Then, we adopt the same Transition Down (TD) scheme proposed in Point Transformer (Zhao et al., 2021). A TD layer contains a set abstraction downsampling scheme, originated from PointNet++ (Qi et al., 2017b), a local graph convolution with kNN connectivity and a local max-pooling layer. We do not adopt a simpler embedding only (for instance, a single MLP) for two reasons. i) We need to lift input point features to the appropriate dimension to transformer blocks, by looking loosely in local region; ii) We need to reduce the cardinality of dense sets for efficient reasoning. We denote each layer of Transition Down operation as $TD(X, P)$, whose output is a new pair of point coordinate and features (X', P') with fewer [cardinality](#) in X' and lifted feature dimension in P' . To match a uniform setting, we add a class token to the tokenized sequence. Later on, this token will not contribute to the segmentation task.

Positional Embedding for Point Clouds We distinguish our positional embedding scheme from any previous work in 3D space. The formula is a simple addition and we state it in equation 8. We adopt only a single MLP to lift up point cloud coordinate X , and then we sum the result with the point features P altogether for tokenizing. We did not require the transformer backbone to adopt any positional embedding components to fit the point cloud modality.

Segmentation Task Head Design For dense semantic segmentation, since we have proposed applying a down-sampling layer, i.e. TD, to the input point cloud, we need to interpolate back to the same input dimension. We adopt the Transition Up(TU) layer in Point Transformer (Zhao et al., 2021) to match TD layers earlier in tokenized scheme. TU layer receives both input coordinate-feature pair from the previous layer as well as the coordinate-feature pair from the same depth TD layer. Overall, the changes we made can be formulated as:

$$\tilde{P} = MLP_2(P + MLP_1(X)); \quad \mathbf{z}_0^{PC} = [\mathbf{x}_{class}; TD(TD(X, \tilde{P}))]; \quad (8)$$

$$\mathbf{y} = h(TU(TU(LN(\mathbf{z}_{L,1:N}), TD(X, \tilde{P})), (X, \tilde{P}))). \quad (9)$$

We refer to Figure 3 as the overall visualized design of our Simple3D-Former for point cloud data. For detail architecture of Simple3D-Former in segmentation, we refer readers to Appendix C.

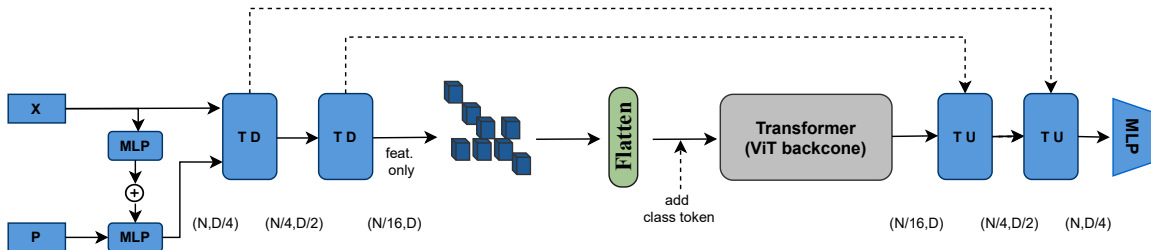


Figure 3: To transfer from a classification backbone into an object part segmentation backbone, we propose some additional, yet easy extensions that fit into 3D data modality. Given input point clouds with its coordinates X , features P , we compose positional information into features first and use a simple MLP to elevate features into $D/4$ dimensions, given D the dimension of backbone. Then we apply two layers of Transition down over pair (X, P) , then feed the abstracted point cloud tokens sequentially into the transformer backbone. To generate the dense prediction. We follow the residual setting and add feature output from TD layers together with the previous layers’ output into a transition up layer. Then we apply a final MLP layer to generate dense object part predictions.

3.2 Incorporating 2D Reasoning Knowledge

The advantage of keeping the backbone transformer unchanged is to utilize the comprehensive learnt model in 2D ViT. Our Simple3D-Former can learn from 2D pretrained tasks thanks to the flexibility of choice of backbone structure, without any additional design within transformer blocks. We treat 2D knowledge as either an initial step of finetuning Simple3D-Former or prior knowledge transferred from a distinguished task. The overall idea is demonstrated in Figure 4.

Pretraining from 2D ViT As shown in Figure 1, we did not change the architecture of transformer backbone. Therefore, one can load transformer backbone weight from 2D-pretrained checkpoints with any difficulty. This is different from a direct 3D Convolutional Kernel Inflation (Shan et al., 2018; Xu et al., 2021) by maintaining the pure reasoning from patch understanding. We observed that one needs to use a small learning rates in first few epochs as a warm-up fine-tuning, to prevent catastrophic forgetting from 2D pretrained ViT. The observation motivates a better transfer learning scheme by infusing the knowledge batch-by-batch.

Retrospecting From 2D Cases by Generalization As we are transferring a model trained on 2D ImageNet to unseen 3D data, retaining the ImageNet domain knowledge is potentially beneficial to the generalized 3D task. Following such a motivation, we require our Simple3D-Former to memorize the representation learned from ImageNet while training on 3D. Therefore, apart from the loss function given in 3d task \mathcal{L}_{3d} , we propose adding the divergence measurement as a proxy guidance during our transfer learning process (Chen et al., 2020b). We fix a pretrained teacher network (teacher ViT in Figure 4). When training

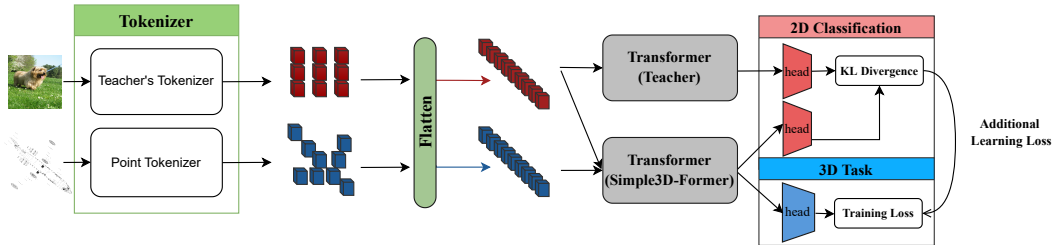


Figure 4: Memorizing 2D knowledge. The teacher network (with all weights fixed) guide the current task by comparing the performance over the pretrained task.

Table 1: Baseline Comparison in 3D Object Classification

Method	Modality	ModelNet40		ScanObjectNN
		mAcc.(%)	OA. (%)	PB-T50-RS OA. (%)
VoxelNet(Maturana & Scherer, 2015)	Voxel	83.0	85.9	-
PointNet(Qi et al., 2017a)	Point	86.2	89.2	68.0
PointNet++(Qi et al., 2017b)	Point	-	91.9	77.9
Perceiver(Jaegle et al., 2021b)	Point	-	85.7	-
DGCNN (Wang et al., 2019b)	Point	90.2	92.2	78.1
Image2Point(Xu et al., 2021)	Voxel	-	89.1	-
Point Transformer(Zhao et al., 2021)	Point	90.6	93.7	81.2
PVT(Zhang et al., 2021)	Point	-	94.0	-
Point-BERT(Yu et al., 2021b)	Point ¹	93.2	-	83.1
Simple3D-Former (ours) ²	Voxel(NI)	82.8	86.5	-
	Voxel(Avg.)	82.4	85.9	-
	Voxel(GE)	84.0	88.0	-
	Point	89.3	92.0	83.1

¹ We report the result with 1024 point sample inputs here to match with other methods.

² NI:Naive Embedding; Avg.: Averaging; GE: Group Embedding.

each mini-batch of 3D data, we additionally bring a mini-batch of images from ImageNet validation set (in batch size M). To generate a valid output class vector, we borrow every part except Transformer blocks from 2D teacher ViT and generate 2D class labeling. We then apply an additional KL divergence to measure knowledge memorizing power, denoted as:

$$\mathcal{L} := \mathcal{L}_{3d} + \lambda \sum_{i=1}^M KL(\mathbf{y}_{teacher} || \mathbf{y}). \quad (10)$$

The original 3d task loss, \mathcal{L}_{3d} with additional KL divergence regularization, forms our teacher-student’s training loss. The vector $\mathbf{y}_{teacher}$ is from 2D teacher ViT output, and \mathbf{y} comes from a same structure as teacher ViT, with the transformer block weight updated as we learn 3D data. In practical implementation, since the teacher ViT is fixed, the hyper-parameter λ depends on the task: see Section 4.

4 Experiments

We test our Simple-3DFormer over three different 3D tasks: object classification, semantic segmentation and object detection. For detailed dataset setup and training implementations, we refer readers to Appendix A.

4.1 3D Object Classification

3D object classification tasks receives a 3D point cloud or 3D voxel as its input and output the object categories. We test 3D classification performance over ModelNet40 (Wu et al., 2015) dataset and ScanObjectNN (Uy et al., 2019) dataset. To generate voxel input of ModelNet40, We use binvoxMin (2004 - 2019); Nooruddin & Turk (2003) to voxelize the data into a 30^3 input. The size 30 follows the standard setup in ModelNet40 setup. We choose to apply Group Embedding scheme as our best Simple3D-Former to compare with existing state-of-the-art methods. We further report the result in Table 1, compared with other state-of-the-art

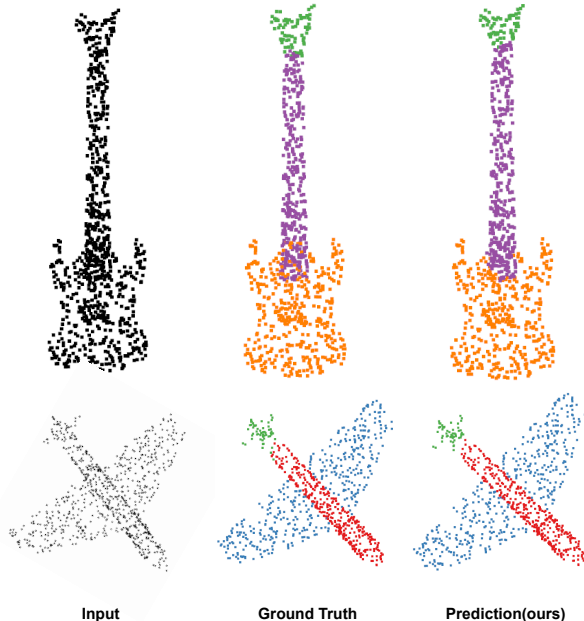


Figure 5: Selective visualizations of point cloud part segmentation.

Table 2: Comparison of 3D segmentation results on the ShapeNetPart and S3DIS dataset.

Method	ShapeNetPartSeg		S3DIS	
	cat. mIoU.(%)	ins. mIoU.(%)	mAcc.(%)	ins. mIoU.(%)
PointNet(Qi et al., 2017a)	80.4	83.7	49.0	41.1
PointNet++(Qi et al., 2017b)	81.9	85.1	-	-
PointCNN(Li et al., 2018)	84.6	86.1	75.6	65.4
DGCNN(Wang et al., 2019b)	82.3	85.1	56.1	-
KPConv(Thomas et al., 2019)	85.1	86.4	72.8	67.1
Point Transformer(Zhao et al., 2021)	83.7	86.6	76.5	70.4
PVT(Zhang et al., 2021)	-	86.5	67.7	61.3
PatchFormer(Cheng et al., 2021)	-	86.7	-	68.1
Simple3D-Former (ours)	83.3	86.0	72.5	67.0

methods over ModelNet40 dataset, and over ScanObjectNN dataset. We optimize the performance of our Simple3D-Former with voxel input by setting up $T = 6$ in equation 7. We finetune with pretrained weight as well as using memorizing regularization equation 10 with M equal to batch size. The classification result of point cloud modality is generated by dropping out two TU layers and passing the class token into a linear classifier head, with the same training setup as ShapeNetV2 case. Our network outperforms previous CNN based designs, and yields a competitive performance compared with 3D transformers. Several prior works observed that adding relative positional encoding within self-attention is important for a performance boost. We appreciate these findings, but claim that a well-pretrained 2D ViT backbone, with real semantic knowledge infused, does assist a simple, unified network to learn across different data modalities. The observation is particularly true over ScanObjectNN dataset, where transformer-enlightened networks outperform all past CNN based networks. Our method, with relatively small parameter space, achieves a similar result compared with Point-BERT.

4.2 3D Point Cloud Segmentation

3D point cloud segmentation is a two-fold task. One receives a point cloud input (either an object or indoor scene scans) and output a class labels per input point within the point cloud. The output simultaneously contains segmentation as well as classification information. Figure 5 is a visual example of object part segmentation task. We report our performance over object part segmentation task in Table 2. The target datasets

Table 3: 3D Detection Result over SUN RGB-D data

Metric	BoxNet	VoteNet	3DETR	3DETR-masked	H3DNet	Simple3D-Former (ours)
AP ₂₅	52.4	58.3	58.0	59.1	60.1	57.6
AP ₅₀	25.1	33.4	30.3	32.7	39.0	32.0

are ShapeNetPart (Yi et al., 2016) dataset and Semantic 3D Indoor Scene dataset, S3DIS (Armeni et al., 2016). We do observe that some articulated designed transformer network, such as Point Transformers (Zhao et al., 2021) and PatchFormer (Cheng et al., 2021) reach the overall best performance by designing their transformer networks to fit 3D data with more geometric priors, while our model bond geometric information only by a positional embedding at tokenization. Nevertheless, our model does not harm the performance and is very flexible in designing. Figure 5 visualizes our Simple3D-Former prediction. The prediction is close to ground truth and it is surprisingly coming from 2D vision transformer backbone without any further geometric-aware infused knowledge. Moreover, the prior knowledge comes only from ImageNet classification task, indicating a good generalization ability within our network.

4.3 3D Object Detection

3D object detection is a pose estimation task. For any given 3D input, one needs to return a 3D bounding box of each detected objects of targeted class. In our experiments we use point cloud input data. We test our simple-3DFormer for SUN RGB-D detection task (Song et al., 2015). We compare our results with BoxNet (Qi et al., 2019), VoteNet (Qi et al., 2019), 3DETR (Misra et al., 2021) and H3DNet (Yin et al., 2020). We follow the experiment setup from Misra et al. (2021): we report the detection performance on the validation set using mean Average Precision (mAP) at IoU thresholds of 0.25 and 0.5, referred to as AP25 and AP50. The result is shown in Table 3 and the evaluation is conducted over the 10 most frequent categories for SUN RGB-D. Even though 3DETR is a simple coupled Transformer Encoder-Decoder coupled system, we have shown that our scheme can achieve similar performance by replacing 3D backbone with our simple3D-Former scheme.

4.4 Ablation Study

Different Performance With/Without 2D Infused Knowledge To justify our Simple3D-Former can learn to generalize from 2D task to 3D task, we study the necessity of prior knowledge for performance boost. We compare the performance among four different settings: i) train without any 2D knowledge; ii) with pretrained 2D ViT weights loaded; iii) with a teacher ViT only, by applying additional 2D tasks and use the loss in equation 10; iv) using both pretraining weights and a teacher ViT.

Results shown in Table 4 reflect our motivation. One does achieve the best performance by not only infusing prior 2D pretraining weight at an early stage, but also getting pay-offs by learning without forgetting prior knowledge. It probably benefits a more complex, large-scale task which is based upon our Simple3D-Former.

Table 4: Power of 2D Prior Knowledge, with 2D projection scheme and evaluated in OA. (%) The performance is tested under ShapeNetV2 and ModelNet40 dataset.

Pretrain Usage	ShapeNetV2	ModelNet40
Without Any 2D Knowledge	82.8	86.5
With 2D pretraining	83.5	86.6
Teacher ViT	84.3	87.6
Pretrain + Teacher ViT	84.5	88.0

Table 5: Power of 2D Prior Knowledge (with teacher ViT) in 3D task, evaluated in cat. mIoU.(%) and ins. mIoU.(%) over ShapeNet Part Segmentation

3D Data Portion	M	cat. mIoU.(%)	ins, mIoU. (%)
25%	0	79.1	83.3
	32	79.4	83.1
	64	79.8	83.6
50%	0	79.5	84.1
	32	79.9	84.0
	64	80.3	84.5
100%	0	81.1	84.6
	32	82.8	85.4
	64	83.1	85.7

Performance in Low-Quantity 3D Data Regime The computation complexity of point cloud data goes up as the number of sample points blows up. Even for a fixed point cloud sampling of 1024 points, it is inefficient to train over the entire dataset. To test the generalization ability of our Simple3D-Former, we perform a test to explore the power of 2D knowledge transferring. We use only a portion of training data in 3D and change the batch size of source task images M at different scales. Result in Table 5 justify the performance over point cloud part segmentation task. Though one needs more data to attain higher accuracy, we found 2D pretrained knowledge offers an accuracy boost. The result indicates a potential joint-training across different data modality and different tasks to find universal transformers with good generalization ability.

4.5 Limitation of our work

Our method challenges the necessity of heavy-lifting design of transformers for 3D tasks. However, a potential drawback of our simple3D-Former is an overlook in 3D-aware only knowledge in the tokenizing process. It has been justified in Point Transformer(Zhao et al., 2021) the layer-wise positional encoding is beneficial for point cloud understanding. While our method is flexible in choosing tokenizer and transformer backbone, the performance might be hindered from a strict fixed transformer structure.

Another concern is that the performance of our method is strongly related with the complexity of selected transformer backbone. Our Simple3D-Former outperforms early-stage point cloud CNN architectures with a total of 29.59G Multiply Add Cumulations(MACs). On the contrary, Point Transformer Zhao et al. (2021) has a total of 36.76G MACs. The detailed model complexity comparison is shown in Appendix B and D. We observe that even with the most complex ViT model (deit-base) we have been testified, we cannot yield the state-of-the-art performance compared with concurrent works. It is in particular true for large indoor scene data (S3DIS) shown in Table 2. How to yield the best trade-off and how the result is different from choice of backbone (especially the embedding dimension) need to be analyzed further by introducing different designs of transformer backbones.

5 Conclusion

We retrospect the development of Vision Transformer and propose a unified version of a 3D transformer, named as Simple3D-Former, that learns from 2D rich-knowledge domain. a 2D ViT can inflate into a 3D ViT, by replacing 2D feature embedding, positional embedding and end-task head layer. Moreover, we justify that 2D domain knowledge helps our model perform better when understanding 3D data and the power of our model can be further strengthened by learning without forgetting. Our experimental result indicates self-attention modules, if learnt from 2D domain knowledge, can be distilled and thereby help the learning 3D object classification, part segmentation and detection tasks under both voxel and point cloud data. In the subsequent work, we hope to explore more versatile combinations of 2D transformer backbones attached with distinguished 3D feature extracting layers, and include complex tasks in large scale datasets.

References

- Hassan Akbari, Linagzhe Yuan, Rui Qian, Wei-Hong Chuang, Shih-Fu Chang, Yin Cui, and Boqing Gong. Vatt: Transformers for multimodal self-supervised learning from raw video, audio and text. *arXiv preprint arXiv:2104.11178*, 2021.
- Iro Armeni, Ozan Sener, Amir R Zamir, Helen Jiang, Ioannis Brilakis, Martin Fischer, and Silvio Savarese. 3d semantic parsing of large-scale indoor spaces. In *Proceedings of the IEEE conference on computer vision and pattern recognition*, pp. 1534–1543, 2016.
- Alexei Baevski and Michael Auli. Adaptive input representations for neural language modeling. In *International Conference on Learning Representations*, 2019. URL <https://openreview.net/forum?id=ByxZX20qFQ>.
- Gedas Bertasius, Heng Wang, and Lorenzo Torresani. Is space-time attention all you need for video understanding? In Marina Meila and Tong Zhang (eds.), *Proceedings of the 38th International Conference on Machine Learning, ICML 2021, 18-24 July 2021, Virtual Event*, volume 139 of *Proceedings of Machine Learning Research*, pp. 813–824. PMLR, 2021. URL <http://proceedings.mlr.press/v139/bertasius21a.html>.
- Nicolas Carion, Francisco Massa, Gabriel Synnaeve, Nicolas Usunier, Alexander Kirillov, and Sergey Zagoruyko. End-to-end object detection with transformers. In *European Conference on Computer Vision*, pp. 213–229. Springer, 2020.
- Mark Chen, Alec Radford, Rewon Child, Jeffrey Wu, Heewoo Jun, David Luan, and Ilya Sutskever. Generative pretraining from pixels. In *International Conference on Machine Learning*, pp. 1691–1703. PMLR, 2020a.
- Wuyang Chen, Zhiding Yu, Zhangyang Wang, and Animashree Anandkumar. Automated synthetic-to-real generalization. In *International Conference on Machine Learning*, pp. 1746–1756. PMLR, 2020b.
- Wuyang Chen, Xianzhi Du, Fan Yang, Lucas Beyer, Xiaohua Zhai, Tsung-Yi Lin, Huizhong Chen, Jing Li, Xiaodan Song, Zhangyang Wang, et al. A simple single-scale vision transformer for object localization and instance segmentation. *arXiv preprint arXiv:2112.09747*, 2021.
- Zhang Cheng, Haocheng Wan, Xinyi Shen, and Zizhao Wu. Patchformer: A versatile 3d transformer based on patch attention. *arXiv preprint arXiv:2111.00207*, 2021.
- Jacob Devlin, Ming-Wei Chang, Kenton Lee, and Kristina Toutanova. BERT: Pre-training of deep bidirectional transformers for language understanding. In *Proceedings of the 2019 Conference of the North American Chapter of the Association for Computational Linguistics: Human Language Technologies, Volume 1 (Long and Short Papers)*, pp. 4171–4186, Minneapolis, Minnesota, June 2019. Association for Computational Linguistics. doi: 10.18653/v1/N19-1423. URL <https://www.aclweb.org/anthology/N19-1423>.
- Alexey Dosovitskiy, Lucas Beyer, Alexander Kolesnikov, Dirk Weissenborn, Xiaohua Zhai, Thomas Unterthiner, Mostafa Dehghani, Matthias Minderer, Georg Heigold, Sylvain Gelly, et al. An image is worth 16x16 words: Transformers for image recognition at scale. *arXiv preprint arXiv:2010.11929*, 2020.
- Nico Engel, Vasileios Belagiannis, and Klaus Dietmayer. Point transformer. *arXiv preprint arXiv:2011.00931*, 2020.
- Hehe Fan, Yi Yang, and Mohan S. Kankanhalli. Point 4d transformer networks for spatio-temporal modeling in point cloud videos. In *Proceedings of the IEEE Conference on Computer Vision and Pattern Recognition*, 2021.
- Hehe Fan, Yi Yang, and Mohan S. Kankanhalli. Point spatio-temporal transformer networks for point cloud video modeling. 2022. doi: 10.1109/TPAMI.2022.3161735.
- Yuxin Fang, Shusheng Yang, Shijie Wang, Yixiao Ge, Ying Shan, and Xinggang Wang. Unleashing vanilla vision transformer with masked image modeling for object detection. *arXiv preprint arXiv:2204.02964*, 2022.

- Rohit Girdhar, Mannat Singh, Nikhila Ravi, Laurens van der Maaten, Armand Joulin, and Ishan Misra. Omnivore: A single model for many visual modalities. *arXiv preprint arXiv:2201.08377*, 2022.
- Tianrui Guan, Jun Wang, Shiyi Lan, Rohan Chandra, Zuxuan Wu, Larry Davis, and Dinesh Manocha. M3detr: Multi-representation, multi-scale, mutual-relation 3d object detection with transformers. *arXiv preprint arXiv:2104.11896*, 2021.
- Meng-Hao Guo, Jun-Xiong Cai, Zheng-Ning Liu, Tai-Jiang Mu, Ralph R Martin, and Shi-Min Hu. Pct: Point cloud transformer. *Computational Visual Media*, 7(2):187–199, 2021.
- Kaiming He, Xinlei Chen, Saining Xie, Yanghao Li, Piotr Dollár, and Ross Girshick. Masked autoencoders are scalable vision learners, 2021.
- Andrew Jaegle, Sebastian Borgeaud, Jean-Baptiste Alayrac, Carl Doersch, Catalin Ionescu, David Ding, Skanda Koppula, Daniel Zoran, Andrew Brock, Evan Shelhamer, et al. Perceiver io: A general architecture for structured inputs & outputs. *arXiv preprint arXiv:2107.14795*, 2021a.
- Andrew Jaegle, Felix Gimeno, Andy Brock, Oriol Vinyals, Andrew Zisserman, and Joao Carreira. Perceiver: General perception with iterative attention. In *International Conference on Machine Learning*, pp. 4651–4664. PMLR, 2021b.
- Alexander Kolesnikov, André Susano Pinto, Lucas Beyer, Xiaohua Zhai, Jeremiah Harmsen, and Neil Houlsby. Uvim: A unified modeling approach for vision with learned guiding codes. *arXiv preprint arXiv:2205.10337*, 2022.
- Abhijit Kundu, Xiaoqi Yin, Alireza Fathi, David Ross, Brian Brewington, Thomas Funkhouser, and Caroline Pantofaru. Virtual multi-view fusion for 3d semantic segmentation. In *European Conference on Computer Vision*, pp. 518–535. Springer, 2020.
- Yanghao Li, Hanzi Mao, Ross Girshick, and Kaiming He. Exploring plain vision transformer backbones for object detection. *arXiv preprint arXiv:2203.16527*, 2022.
- Yangyan Li, Rui Bu, Mingchao Sun, Wei Wu, Xinhan Di, and Baoquan Chen. Pointcnn: Convolution on x-transformed points. *Advances in neural information processing systems*, 31:820–830, 2018.
- Kevin Lin, Lijuan Wang, and Zicheng Liu. End-to-end human pose and mesh reconstruction with transformers. In *Proceedings of the IEEE/CVF Conference on Computer Vision and Pattern Recognition*, pp. 1954–1963, 2021.
- Yueh-Cheng Liu, Yu-Kai Huang, Hung-Yueh Chiang, Hung-Ting Su, Zhe-Yu Liu, Chin-Tang Chen, Ching-Yu Tseng, and Winston H Hsu. Learning from 2d: Pixel-to-point knowledge transfer for 3d pretraining. *arXiv preprint arXiv:2104.04687*, 2021a.
- Ze Liu, Yutong Lin, Yue Cao, Han Hu, Yixuan Wei, Zheng Zhang, Stephen Lin, and Baining Guo. Swin transformer: Hierarchical vision transformer using shifted windows. *arXiv preprint arXiv:2103.14030*, 2021b.
- Shengjie Luo, Tianlang Chen, Yixian Xu, Shuxin Zheng, Tie-Yan Liu, Liwei Wang, and Di He. One transformer can understand both 2d & 3d molecular data. *arXiv preprint arXiv:2210.01765*, 2022.
- Jiageng Mao, Yujing Xue, Minzhe Niu, Haoyue Bai, Jiashi Feng, Xiaodan Liang, Hang Xu, and Chunjing Xu. Voxel transformer for 3d object detection. In *Proceedings of the IEEE/CVF International Conference on Computer Vision*, pp. 3164–3173, 2021.
- Daniel Maturana and Sebastian Scherer. Voxnet: A 3d convolutional neural network for real-time object recognition. In *2015 IEEE/RSJ International Conference on Intelligent Robots and Systems (IROS)*, pp. 922–928, 2015. doi: 10.1109/IROS.2015.7353481.
- Patrick Min. binvox. <http://www.patrickmin.com/binvox> or <https://www.google.com/search?q=binvox>, 2004 - 2019. Accessed: yyyy-mm-dd.

- Ishan Misra, Rohit Girdhar, and Armand Joulin. An End-to-End Transformer Model for 3D Object Detection. In *ICCV*, 2021.
- Fakir S. Nooruddin and Greg Turk. Simplification and repair of polygonal models using volumetric techniques. *IEEE Transactions on Visualization and Computer Graphics*, 9(2):191–205, 2003.
- Niki Parmar, Ashish Vaswani, Jakob Uszkoreit, Lukasz Kaiser, Noam Shazeer, Alexander Ku, and Dustin Tran. Image transformer. In *International Conference on Machine Learning*, pp. 4055–4064. PMLR, 2018.
- Charles R Qi, Hao Su, Kaichun Mo, and Leonidas J Guibas. Pointnet: Deep learning on point sets for 3d classification and segmentation. In *Proceedings of the IEEE conference on computer vision and pattern recognition*, pp. 652–660, 2017a.
- Charles R. Qi, Li Yi, Hao Su, and Leonidas J. Guibas. Pointnet++: Deep hierarchical feature learning on point sets in a metric space. In *Proceedings of the 31st International Conference on Neural Information Processing Systems, NIPS’17*, pp. 5105–5114, Red Hook, NY, USA, 2017b. Curran Associates Inc. ISBN 9781510860964.
- Charles R Qi, Or Litany, Kaiming He, and Leonidas J Guibas. Deep hough voting for 3d object detection in point clouds. In *proceedings of the IEEE/CVF International Conference on Computer Vision*, pp. 9277–9286, 2019.
- Mehdi SM Sajjadi, Henning Meyer, Etienne Pot, Urs Bergmann, Klaus Greff, Noha Radwan, Suhani Vora, Mario Lučić, Daniel Duckworth, Alexey Dosovitskiy, et al. Scene representation transformer: Geometry-free novel view synthesis through set-latent scene representations. In *Proceedings of the IEEE/CVF Conference on Computer Vision and Pattern Recognition*, pp. 6229–6238, 2022.
- Hongming Shan, Yi Zhang, Qingsong Yang, Uwe Kruger, Mannudeep K Kalra, Ling Sun, Wenxiang Cong, and Ge Wang. 3-d convolutional encoder-decoder network for low-dose ct via transfer learning from a 2-d trained network. *IEEE transactions on medical imaging*, 37(6):1522–1534, 2018.
- Shuran Song, Samuel P Lichtenberg, and Jianxiong Xiao. Sun rgb-d: A rgb-d scene understanding benchmark suite. In *Proceedings of the IEEE conference on computer vision and pattern recognition*, pp. 567–576, 2015.
- Hang Su, Subhransu Maji, Evangelos Kalogerakis, and Erik Learned-Miller. Multi-view convolutional neural networks for 3d shape recognition. In *Proceedings of the IEEE international conference on computer vision*, pp. 945–953, 2015.
- Hugues Thomas, Charles R Qi, Jean-Emmanuel Deschaud, Beatriz Marcotegui, François Goulette, and Leonidas J Guibas. Kpconv: Flexible and deformable convolution for point clouds. In *Proceedings of the IEEE/CVF International Conference on Computer Vision*, pp. 6411–6420, 2019.
- Hugo Touvron, Matthieu Cord, Matthijs Douze, Francisco Massa, Alexandre Sablayrolles, and Hervé Jégou. Training data-efficient image transformers & distillation through attention. In *International Conference on Machine Learning*, pp. 10347–10357. PMLR, 2021.
- Mikaela Angelina Uy, Quang-Hieu Pham, Binh-Son Hua, Duc Thanh Nguyen, and Sai-Kit Yeung. Revisiting point cloud classification: A new benchmark dataset and classification model on real-world data. In *International Conference on Computer Vision (ICCV)*, 2019.
- Ashish Vaswani, Noam Shazeer, Niki Parmar, Jakob Uszkoreit, Llion Jones, Aidan N Gomez, Łukasz Kaiser, and Illia Polosukhin. Attention is all you need. In I. Guyon, U. V. Luxburg, S. Bengio, H. Wallach, R. Fergus, S. Vishwanathan, and R. Garnett (eds.), *Advances in Neural Information Processing Systems*, volume 30. Curran Associates, Inc., 2017a. URL <https://proceedings.neurips.cc/paper/2017/file/3f5ee243547dee91fbd053c1c4a845aa-Paper.pdf>.
- Ashish Vaswani, Noam Shazeer, Niki Parmar, Jakob Uszkoreit, Llion Jones, Aidan N Gomez, Łukasz Kaiser, and Illia Polosukhin. Attention is all you need. In *Advances in neural information processing systems*, pp. 5998–6008, 2017b.

- Peihao Wang, Wenqing Zheng, Tianlong Chen, and Zhangyang Wang. Anti-oversmoothing in deep vision transformers via the fourier domain analysis: From theory to practice. *arXiv preprint arXiv:2203.05962*, 2022.
- Qiang Wang, Bei Li, Tong Xiao, Jingbo Zhu, Changliang Li, Derek F. Wong, and Lidia S. Chao. Learning deep transformer models for machine translation. In *Proceedings of the 57th Annual Meeting of the Association for Computational Linguistics*, pp. 1810–1822, Florence, Italy, July 2019a. Association for Computational Linguistics. doi: 10.18653/v1/P19-1176. URL <https://aclanthology.org/P19-1176>.
- Yue Wang, Yongbin Sun, Ziwei Liu, Sanjay E Sarma, Michael M Bronstein, and Justin M Solomon. Dynamic graph cnn for learning on point clouds. *Acm Transactions On Graphics (tog)*, 38(5):1–12, 2019b.
- Zhirong Wu, Shuran Song, Aditya Khosla, Fisher Yu, Linguang Zhang, Xiaoou Tang, and Jianxiong Xiao. 3d shapenets: A deep representation for volumetric shapes. In *Proceedings of the IEEE conference on computer vision and pattern recognition*, pp. 1912–1920, 2015.
- Chenfeng Xu, Shijia Yang, Bohan Zhai, Bichen Wu, Xiangyu Yue, Wei Zhan, Peter Vajda, Kurt Keutzer, and Masayoshi Tomizuka. Image2point: 3d point-cloud understanding with pretrained 2d convnets. *arXiv preprint arXiv:2106.04180*, 2021.
- Yao Yao, Zixin Luo, Shiwei Li, Jingyang Zhang, Yufan Ren, Lei Zhou, Tian Fang, and Long Quan. Blendedmvs: A large-scale dataset for generalized multi-view stereo networks. *Computer Vision and Pattern Recognition (CVPR)*, 2020.
- Li Yi, Vladimir G Kim, Duygu Ceylan, I-Chao Shen, Mengyan Yan, Hao Su, Cewu Lu, Qixing Huang, Alla Sheffer, and Leonidas Guibas. A scalable active framework for region annotation in 3d shape collections. *ACM Transactions on Graphics (ToG)*, 35(6):1–12, 2016.
- Junbo Yin, Jianbing Shen, Chenye Guan, Dingfu Zhou, and Ruigang Yang. Lidar-based online 3d video object detection with graph-based message passing and spatiotemporal transformer attention. In *Proceedings of the IEEE/CVF Conference on Computer Vision and Pattern Recognition*, pp. 11495–11504, 2020.
- Xumin Yu, Yongming Rao, Ziyi Wang, Zuyan Liu, Jiwen Lu, and Jie Zhou. Pointtr: Diverse point cloud completion with geometry-aware transformers. In *Proceedings of the IEEE/CVF International Conference on Computer Vision*, pp. 12498–12507, 2021a.
- Xumin Yu, Lulu Tang, Yongming Rao, Tiejun Huang, Jie Zhou, and Jiwen Lu. Point-bert: Pre-training 3d point cloud transformers with masked point modeling. *arXiv preprint arXiv:2111.14819*, 2021b.
- Cheng Zhang, Haocheng Wan, Shengqiang Liu, Xinyi Shen, and Zizhao Wu. Pvt: Point-voxel transformer for 3d deep learning. *arXiv preprint arXiv:2108.06076*, 2021.
- Hengshuang Zhao, Li Jiang, Jiaya Jia, Philip H.S. Torr, and Vladlen Koltun. Point transformer. In *Proceedings of the IEEE/CVF International Conference on Computer Vision (ICCV)*, pp. 16259–16268, October 2021.
- Daquan Zhou, Bingyi Kang, Xiaojie Jin, Linjie Yang, Xiaochen Lian, Zihang Jiang, Qibin Hou, and Jiashi Feng. Deepvit: Towards deeper vision transformer. *arXiv preprint arXiv:2103.11886*, 2021.

A Dataset Setup and Implementation Details

A.1 3D Object Classification

Dataset Setup ModelNet40 consists of 12311 samples with 9843 training samples and 2468 test samples. It contains 40 classes in total. The original data is aligned and in point-cloud format. ScanObjectNN contains 2902 CAD objects with background knowledge provided in point cloud as well. It contains 15 classes in total. We apply our model over the augmented PB_T50_RS batch samples, in which bounding boxes of objects can shift up to 50% and objects are perturbed with rotation and scaling, resulting in 14510 total input train/test

samples. We follow the standard sampling scheme to generate a subset of 1024 points for every point cloud model in both datasets. We additionally use ShapeNetV2[47] to testify our Simple3D-Former for voxel input as well. For details on ShapeNetV2 classification, we refer readers to Appendix B.

Implementation Details We use one TITAN A100 for training. For voxel classification task, we use the Adam optimizer with an initial warm-up at starting learning rate of 0.01, which is decayed by a factor of 0.5 every 20 epochs. The batch size is set to 64. We trained 100 epochs in total. The hyperparameter λ is set to 0.1 back in (10). We evaluate mean of class-wise accuracy (mAcc), and overall point-wise accuracy (OA). The voxel embedding E_V we choose is a single convolutional layer with kernel size of T and stride T to generate tokenized sequence and remain simple. The pretrained knowledge comes from DeIT. The experiment is conducted with DeIT-base backbone with ImageNet-1K pretraining of image size 224. We justify the ablation study for choosing backbones and appropriate positional embedding parameters for optimal performance. In addition, we show that optimal performance is obtained by using not only ViT backbone but pretrained 2D knowledge and the help of memorizing 2D tasks. We report the result in Appendix B accordingly.

A.2 3D Point Cloud Segmentation

Dataset Setup For object part segmentation, we test over ShapeNetPart dataset, containing 16,881 pre-aligned shapes with dense labeling of 50 different parts over 16 distinguished categorical objects. We sample 1024 points for every point cloud model with standard process. We evaluate our Simple3D-Former over semantic indoor scene semantic segmentation dataset, S3DIS, as well. S3DIS contains 5 large-scale indoor scans with 12 semantic elements. We use area 5 as the test case while the remaining areas are treated as training data. We sample 4096 points for every partitioned indoor scene with standard process.

Implementation Details The training is conducted on one TITAN A100. For object part segmentation task, we use the SGD optimizer with an initial learning rate of 0.05, which is decayed by a factor of 0.1 every 100 epochs. The batch size is set to 64. We trained our Simple3D-Former up-to 300 epochs. For semantic segmentation task, we use the SGD optimizer with an initial learning rate of 0.1, which is decayed by a factor of 0.5 every 20 epochs. We trained 100 epochs with batch size 8. We use DeIT-base as the backbone ViT for both tasks. The hyperparameter λ is set to 0.1 back in equation 10. We evaluate categorical mean intersection over union (cat. mIOU.) and instance mean intersection over union (ins. mIOU.) respectively for ShapeNetPart dataset while we report the mean accuracy and instance mean intersection over union in S3DIS dataset.

A.3 3D Point Cloud Object Detection

Dataset Setup We apply our Simple3D-Former onto a standard 3D indoor detection benchmark, SUN RGB-D (v1). SUN RGB-D contains 5000 training samples with oriented bounding box annotations while KITTI dataset contains 7518 raw 3d input.

Implementation Details To justify our simple3D-Former can be embedded naturally into a detection model’s 3D backbone, we modify 3DETR’s backbone into our version, while keep the decoder head unchanged. The training is conducted on one TITAN A100 and trained over 1080 epochs. Detailed architecture of Simple3D-Former backbone used in detection task is explained in Appendix C.

B More Classification Result With Voxel Input

ShapeNetV2 dataset contains 52456 samples from 55 categories and we use a fixed 80% – 20% train-test split throughout our experiments. The voxel data is of size 128^3 . Note that ShapeNetV2 is evaluated only when we determine which Simple3D-Former setup optimizes the performance over voxel data.

It has been explored in 2D ViT the relationship between the size of patches and the classification accuracy over image dataset. There is no such prior belief in 3D voxel data, so we test our Simple3D-Formers under different settings to find the optimal scheme. For point cloud input, we fix our model all from the beginning.

Table 6: Performance of Different Simple-3DFormer Design on ShapeNetV2 Classification evaluated on OA. (%), either with pretrained 2D ViT weight guidance (W P.) or without pretrained 2D ViT guidance (W/O P.).

Scheme	Token Length	Naive Transformer	
		W P.	W/O P.
Naive Inflation	8 by 8 by 8	83.1	79.8
2D Projection	8 by 8	83.6	82.3
Group Embedding	8 by 8	85.0	84.9
Naive Inflation	14 by 14 by 14	85.5	85.5
2D Projection	14 by 14	83.5	82.8
Group Embedding	14 by 14	87.6	86.8

Table 6 shows the preliminary result. We test under two different cell size settings: $T = 16$ (8 cells per axis) and $T = 9^1$ (14 cells per axis) in equation 4, equation 5 and equation 7. Among all configurations, Group Embedding outperforms Naive Inflation and 2D Projection. More importantly, the pretraining weight adopted in transformer backbone before training over 3D data does help to improve the accuracy of object classification. Another observation is that the size of token sequence affects the result as well. A 9^3 cell yields more semantic meaning compare to that of a 16^3 cell, which neglects too many local connections. Hence, in the following experiments over voxel data,

We further justify that among all transformer backbone mimic from 2D ViT siblings, DeiT-base attains optimal performance. The result is shown in Table 7.

Table 7: Different 2D ViT backbone performance and complexity comparison. The table shows our Simple3DFormer under Group Embedding setup.

Backbone Name	ImageNet(2D)	ModelNet40(3D)		
	Param. (M)	FLOPs (G)	Param. (M)	OA. (%)
DeiT-tiny	5	0.28	5	84.5
DeiT-small	22	1.12	21	86.7
DeiT-base	86	4.46	85	88.0

Different Performance Under Particular Ordering When discussing 2D Projection tokenized scheme for voxel data, we implicitly assume we project along Z -dim. We show that we are not biased from the choice of ordering. Table 8 explains different result of particular ordering in 2D Projection scheme, in both ShapeNetV2 and ModelNet40 dataset. We denote the ordering XYZ as the normal input order, where Z -dim data is projected or grouped. Similarly, YZX refers to the X -dim data projection and ZXY refers to the Y -dim data projection. The result indicates the optimal choice of projection is dataset dependent, but the performance is optimal further when considering group embedding scheme.

Table 8: Performance under different ordering of input voxels, with 2D Projection scheme and evaluated in OA. (%)

Projection View	ShapeNetV2	ModelNet40
XYZ	83.6	82.1
YZX	84.5	83.2
ZXY	81.9	84.3

C Detailed architecture of Simple3D-Former In Point Cloud Modality

Simple3D-Former for Part Segmentation Task The overall Simple3D-Former of point cloud segmentation has a different design of data tokenizer and downstream head (to produce information not from class tokens). In point tokenizer part, two layers of point set abstractions are applied. The Transition Down (TD) layer comes from Point Transformer. A TD layer contains a set abstraction downsampling scheme, originated from PointNet++, a local graph convolution with kNN connectivity, and a local max-pooling layer.

¹For $T = 9$ Group Embedding scheme, we use batch size of 32 instead.

Rather than adding relative positional embedding in attention layers as most 3d-aware transformers did, we propose to add the relative positional embedding in local convolution layers in pointnet++ skeleton (i.e. PointSetAbstraction operation in PointNet++), to avoid artificial design in transformer attention modules, but incorporate local embeddings beforehand. Each TD layer reduces the number of points by 4 with a $2x$ scale-up of the embedding dimension. The newly distilled point tokenized sequence is then fed into the ViT backbone. The Transition Up (TU) layer comes from Point Transformer as well. It interpolates over the original point coordinates by neighboring features and scales down the embedding dimension by 2. TU module also contains a residual block that adds the point feature vectors back in the corresponding TD layer, resulting in a U-Net architecture. We provide code snippets in Listing 1 and 2 for readers to match the practical implementation with Figure 3.

Simple3D-Former for 3D Detection Task In our 3D detection experiment, we replace 3DETR’s transformer encoder structure into our Simple3D-Former design, and generate the output head with same structure as in 3detr, and fix other part to show the flexibility of our design.

```

1
2 self.transition_downs = nn.ModuleList()
3 for i in range(2):
4     channel = self.embed_dim // 4 * 2 ** (i+1)
5     self.transition_downs.append(TransitionDown(npoints // 4 ** i, nneighbor, [channel // 2
6         + 3, channel, channel]))
7
8 self.transition_ups = nn.ModuleList()
9 for i in reversed(range(2)):
10    channel = self.embed_dim // 4 * 2 ** i
11    self.transition_ups.append(TransitionUp(channel * 2, channel, channel))
12
13 self.fc1 = nn.Sequential(
14     nn.Linear(d_points, self.embed_dim // 4),
15     nn.ReLU(),
16     nn.Linear(self.embed_dim // 4, self.embed_dim // 4)
17 )
18 self.fc_pos_embed = nn.Sequential(
19     nn.Linear(3, self.embed_dim // 4),
20     nn.ReLU(),
21     nn.Linear(self.embed_dim // 4, self.embed_dim // 4)
22 )

```

Listing 1: Code Snippet to define TD/TU layers and two MLPs

```

1 def forward_features(self, x):
2     xyz, f = x[..., :3], self.fc1(x)
3     f = self.pos_drop(f + self.fc_pos_embed(xyz))
4
5     xyz_0, points_0 = ...
6     self.transition_downs[0](xyz, f)
7     xyz_1, points_1 = ...
8     self.transition_downs[1](xyz_0, points_0)
9     x = points_1
10
11     # Add dummy class tokens to mimic ViT’s style
12     cls_token = self.cls_token.expand(x.shape[0], -1, -1)
13     x = torch.cat((cls_token, x), dim=1)
14
15     for blk in self.blocks:
16         x = blk(x)
17     x = self.norm(x)
18     x = x[:, 1:]
19     x = self.transition_ups[0](xyz_1, x, xyz_0, points_0)
20     x = self.transition_ups[1](xyz_0, x, xyz, f)
21     return x.mean(1)

```

Listing 2: Code Snippet in forward function

D Different Point Cloud Simple3D-Former Design

We additionally show different results regarding the number of TD/TU coupled layers as the ablation study of Simple3D-Former structure. Note that if TD/TU layer number is 0, only a MLP layer is applied to lift input point cloud features and another MLP is applied to encode absolute positions. Moreover, we fix two MLP layers back in Eqn. (10) to have the same output dimension for a reasonable comparison, when testing with 0 or 1 layer TD/TU setting. For 2 layer TD/TU setup, the dimension of MLP is changing according to the embedding dimension $D/4$ based on different choices of backbones: DeIT-tiny, $D = 192$; DeIT-small, $D = 384$; DeIT-base, $D = 768$.

As TD layer scales up the embedding dimension of point vectors while reducing the size of tokenized sequence, different ViT backbones, when equipped with same number of TD/TU layers, have different scalings. The experiment setup is the same as described in Section 4.2, with $M = 64$ for 2D knowledge infusing. All setups applied pretrained weight from the corresponding backbones as well.

Table 9 shows the result regarding different TD/TU layers. We found that by introducing point abstraction, the performance of a 2D pretrained ViT backbone can be further improved compared with MLP only setup (0 TD/TU layers), with the total computational cost relatively lower. This reflects the claim back in Section 3, where we point out the necessity of point cloud data modality modification to fit into the universal transformer backbone. Our Simple3D-Former can adapt from the change of data modality and obtain a good result, compare with CNN-based schemes.

Table 9: Different Simple3D-Formers’ performance over part segmentation task, evaluated in cat. mIoU. (%), ins. mIoU. (%) and MACs. (G).

# of TD/TU Layers	ShapeNetPart		
	cat. mIoU. (%)	ins. mIoU. (%)	MACs. (G)
0 (DeIT-tiny)	81.7	84.7	5.53
1 (DeIT-small)	82.9	85.1	6.53
1 (DeIT-base)	82.5	84.9	26.04
2 (DeIT-tiny)	82.2	84.7	1.87
2 (DeIT-small)	82.5	84.7	7.42
2 (DeIT-base)	83.1	85.7	29.59